Fast Shape Optimization of Antennas Using Model Order Reduction

Yuki Sato[1], Felipe Campelo[2] and Hajime Igarashi[1], *Member IEEE*

[1]Graduate School of Information Science and Technology, Hokkaido University, 060-0814 Sapporo, Japan
[2] Universidade Federal de Minas Gerais, Departamento de Engenharia Eletrica, Belo Horizonte 31270-901, Brazil.

This paper presents a fast shape optimization method for antennas using proper orthogonal decomposition(POD)-based model order reduction (MOR). In this method, the finite element region is subdivided into design and ambient regions. The former includes antennas whose shapes are optimized, while the latter includes air and the perfect matched layer. Since the EM fields significantly changes in the design region during the optimization process, POD-based MOR is only applied to the ambient region. Moreover, MOR for both shape and frequency responses is performed for optimization of wideband antennas. It is shown that the present method can effectively reduce the computational time without deteriorating performance in the optimization.

***Index Terms*—Model order reduction, finite element method, shape optimization, antenna.**

I. Introduction

In recent years, small and wideband antennas for radio frequency identification (RFID) have been developed using shape optimization [1]-[3]. When using population-based optimization methods such as genetic algorithm (GA) and immune algorithm, we must evaluate fitness of many individuals with computational electromagnetic methods such as finite element method (FEM), finite-difference time-domain method and moment method. Therefore, the optimization processes require long computational time. We need fast computational methods, therefore, to perform the antenna optimization effectively.

Model order reduction (MOR) [4]-[8] is one of the promising methods to reduce the computational time in the optimization processes as MOR technique can effectively reduce the degree of freedom (DoF) of the original system. The parametric MOR (PMOR) has been proposed to reduce the computational time for optimization [4]. In PMOR, the unknowns are interpolated in the tensor grid which spans in parameter domain. PMOR has been shown effective for optimization problems concerning guided waves. The dimension of tensor grid in this method, however, increases with the number of design parameters.

The authors have proposed a fast optimization method using MOR based on proper orthogonal decomposition (POD) for magnetostatic problems [8]. In this method, we snapshot the magnetostatic fields for different device shapes during the preprocessing of optimization. Because magnetic fields inside and near the optimization object strongly depend on its shape, we need large number of snapshots to have accurate results. To circumvent this problem, we subdivide the analysis domain into design and ambient regions. The former includes optimization objects, while the latter surrounds the former region. MOR is applied only to the ambient region while the original equation is solved in the design region. Note here that we do not have to increase the number of snapshots even if the number of design parameters increases. The present method, therefore, can be applied to optimization problems with many DoFs. The magnetostatic optimization problems have successfully been solved by this method at reduced computational burden. However, it remains unclear if this method is valid for antennas and other high-frequency devices in unbounded region because air and absorbing region for open boundary have to be properly model by the MOR technique.

In this paper, the fast optimization method using POD-based MOR is applied to shape optimization of antennas whose property is analyzed by FEM. Moreover, in order to accelerate the optimization of wideband antennas, we propose novel POD-based MOR in which we snapshot EM fields for different object shapes and frequencies in the target band. In this paper, this method is applied to optimization of meander line antenna (MLA) and spiral planar antenna (SPA) which are used for RFID system. It is shown that this method effectively reduces computational time in the optimization processes.

Manuscript received May 23, 2014. Corresponding author: Y. Sato (e-mail: yukisato@em-si.eng.hokudai.ac.jp).
Digital Object Identifier inserted by IEEE

II. Antenna analysis

We use FEM to evaluate antenna characteristic, in which we employ perfect matched layer (PML) [9][10] on the open boundaries. The governing equation for antenna analysis is expressed by

$$\mathrm{rot}(\mu\Lambda(\omega))^{-1}\cdot\mathrm{rot}\boldsymbol{A}-\omega^2\varepsilon\Lambda(\omega)\boldsymbol{A}=\boldsymbol{J} \tag{1}$$

where

$$\Lambda(\omega)=\frac{s_y s_z}{s_x}\hat{x}\hat{x}+\frac{s_y s_z}{s_x}\hat{y}\hat{y}+\frac{s_y s_z}{s_x}\hat{z}\hat{z} \tag{2}$$

$$s_\varsigma=1+\frac{\sigma_\varsigma}{\mathrm{j}\omega}\ (\varsigma=x,y,z) \tag{3}$$

and $\boldsymbol{A}$, $\boldsymbol{J}$, μ, σ, ε and ω are vector potential, current density, magnetic permeability, conductivity, permittivity and angular frequency. Applying the Galerkin method to eq. (1), we obtain FE equation

$$\sum_j A_j\int_V(\mathrm{rot}\,\boldsymbol{N}_i\cdot(\mu\Lambda(\omega))^{-1}\cdot\mathrm{rot}\,\boldsymbol{N}_j-\omega^2\boldsymbol{N}_i\cdot\varepsilon\Lambda(\omega)\cdot\boldsymbol{N}_j)\mathrm{d}V=\int_V\boldsymbol{N}_i\cdot\boldsymbol{J}\mathrm{d}V \tag{4}$$

where $\boldsymbol{N}_i$ is the vector interpolation function. Equation (4) which includes the complex symmetric matrix is solved using the ICCG method.

III. Model Order Reduction for Optimization

A. Optimization of single frequency antennas

Let us consider optimization of antenna shapes operated at a single frequency *f*. For the optimization, we solve eq.(4) for different shape parameters $\boldsymbol{d}_1$, $\boldsymbol{d}_2$, ..., $\boldsymbol{d}_s$ at *f*. Now eq. (4) is expressed by

$$\begin{bmatrix} \mathrm{K}_{11}(\boldsymbol{d}) & \mathrm{K}_{21} \\ \mathrm{K}_{12} & \mathrm{K}_{22} \end{bmatrix} \begin{bmatrix} \boldsymbol{a}_1(\boldsymbol{d}) \\ \boldsymbol{a}_2 \end{bmatrix} = \begin{bmatrix} \boldsymbol{b}_1(\boldsymbol{d}) \\ \boldsymbol{b}_2 \end{bmatrix} \quad (5)$$

where $\boldsymbol{a}_1 \in \mathbb{C}^{(n-l)}$ and $\boldsymbol{a}_2 \in \mathbb{C}^{l}$ are solutions to eq. (4) in the design and ambient region, *n* and *l* are the number of unknowns in the whole and ambient regions, respectively. Moreover, the suffixes 1 and 2 in $\mathrm{K}_{11}(\boldsymbol{u}_i) \in \mathbb{C}^{(n-l)\times(n-l)}$, $\mathrm{K}_{12} \in \mathbb{C}^{(n-l)\times l}$, $\mathrm{K}_{21} \in \mathbb{C}^{l\times(n-l)}$ and $\mathrm{K}_{21} \in \mathbb{C}^{l\times l}$ represent the design and ambient regions. In proposed POD-based MOR, singular value decomposition (SVD) is only applied to the data matrix

$$\mathrm{X} = \left[\boldsymbol{a}_2(\boldsymbol{d}_1) \quad \boldsymbol{a}_2(\boldsymbol{d}_2) \quad \cdots \quad \boldsymbol{a}_2(\boldsymbol{d}_s)\right] \in \mathbb{C}^{l\times s}. \quad (6)$$

which contains the EM variables in the ambient region. SVD results in

$$\mathrm{X} = \mathrm{U}\Sigma\mathrm{V}^* = \sigma_1\boldsymbol{u}_1\boldsymbol{v}_1^* + \sigma_2\boldsymbol{u}_2\boldsymbol{v}_2^* + \cdots + \sigma_s\boldsymbol{u}_s\boldsymbol{v}_s^* \quad (7)$$

where $\boldsymbol{u}_k$ and $\boldsymbol{v}_k$ are the eigenvectors of the variance-covariance matrix XX^* and its Hermitian conjugate $\mathrm{X}^*\mathrm{X}$, respectively and σ_k, k=1,2,…,s are the singular values which correspond to the square root of the eigenvalues of XX^*. The unknown $\boldsymbol{a}_2$ is expressed by the linear combination of the column vectors in U. The condition of the reduced matrix would deteriorate when we use too many column vectors as the basis vectors. Hence, we have to use appropriate number of basis vectors to have good convergence in solution of the reduced system. For this reason, we determine the adequate number of the columns from the contribution ratio defined by

$$\eta \le \frac{\sigma_1 + \cdots + \sigma_r}{\sigma_1 + \sigma_2 + \cdots + \sigma_s} \quad (8)$$

where η is the prescribed contribution ratio. On the basis of the condition (8), we redefine transformation matrix as

$$\mathrm{U}' = \left[\boldsymbol{u}_1 \quad \boldsymbol{u}_2 \quad \cdots \quad \boldsymbol{u}_r\right] \quad (9)$$

where $r \ll l$. The variable $\boldsymbol{a}_2$ is now expressed by the reduced unknowns via the transformation matrix U' as

$$\boldsymbol{a}_2 = \mathrm{U}'\boldsymbol{y} \quad (10)$$

where $\boldsymbol{y} \in \mathbb{C}^s$. Substituting eq. (10) to eq. (5), we can obtain the reduced equation

$$\begin{bmatrix} \mathrm{K}_{11}(\boldsymbol{d}) & \mathrm{K}_{12}\mathrm{U}' \\ \mathrm{U}'^t\mathrm{K}_{21} & \mathrm{U}'^t\mathrm{K}_{22}\mathrm{U}' \end{bmatrix} \begin{bmatrix} \boldsymbol{a}_1 \\ \boldsymbol{y} \end{bmatrix} = \begin{bmatrix} \boldsymbol{b}_1(\boldsymbol{d}) \\ \mathrm{U}'^t\boldsymbol{b}_2 \end{bmatrix} \quad (11)$$

As DoF of $\boldsymbol{a}_2$ is reduced from *l* to *r*, eq. (11) can be solved much faster than eq. (5).

B. Optimization of wideband antennas

We consider now optimization of wideband antennas. For analysis of the antenna characteristics in the frequency band of interest, there are two approaches; we perform the time-domain analysis and then carry out the Fourier transform, or we perform frequency sweep. We choose here the latter, to which a natural extension of the POD-based MOR mentioned in A can be applied. We solve eq.(5) for different shape parameters $\boldsymbol{d}_1$, $\boldsymbol{d}_2$, ..., $\boldsymbol{d}_s$ at sampling frequencies f_1, f_2,...,f_t to obtain the data matrix

$$\hat{\mathrm{X}} = \left[\boldsymbol{a}_2(\boldsymbol{d}_1, f_1) \quad \cdots \quad \boldsymbol{a}_2(\boldsymbol{d}_i, f_j) \quad \cdots \quad \boldsymbol{a}_2(\boldsymbol{d}_s, f_t)\right] \in \mathbb{C}^{l\times st} \quad (12)$$

where i=1,…s, j=1,…t. SVD is applied to the data matrix to obtain

$$\hat{\mathrm{X}} = \hat{\mathrm{U}}\hat{\Sigma}\hat{\mathrm{V}}^* = \hat{\sigma}_1\hat{\boldsymbol{u}}_1\hat{\boldsymbol{v}}_1^* + \hat{\sigma}_2\hat{\boldsymbol{u}}_2\hat{\boldsymbol{v}}_2^* + \cdots + \hat{\sigma}_{s\times t}\hat{\boldsymbol{u}}_{s\times t}\hat{\boldsymbol{v}}_{s\times t}^* \quad (13)$$

From (8), we can redefine transformation matrix as

$$\hat{\mathrm{U}}' = \left[\boldsymbol{u}_1 \quad \boldsymbol{u}_2 \quad \cdots \quad \boldsymbol{u}_r\right] \quad (14)$$

Finally, DoF of eq. (5) is reduced using the transformation matrix (14) in the POD-based MOR for the optimization of wideband antennas.

IV. Numerical Results

A. Meander Line Antenna

1) Accuracy and Computational Time

Figure 1 shows the analysis domain which includes a MLA on the green plane. We assume that the MLA is operated at a single frequency. The shape of MLA is expressed by an array of the antenna edge length [1]. The domain is subdivided into design and ambient regions. The former includes MLA, while the latter includes air and PML. The DoFs in the design and ambient regions are 41953 and 934406, respectively. To evaluate accuracy and computational cost of this method, we analyze 50 MLAs of different shapes using present POD-based MOR in which number of snapshots is *s*=30 and number of basis vectors is *r*=20 and 30. The 934406 DoFs in the ambient region are reduced to 20 or 30 by POD-based MOR. The analysis error is defined by

$$\mathrm{error} = \frac{\left\|Z_{\mathrm{in}} - Z_{\mathrm{in\_MOR}}\right\|_2}{\left\|Z_{\mathrm{in}}\right\|_2} \times 100\,[\%] \quad (15)$$

where Z_{in} and $Z_{\mathrm{in\_MOR}}$ denote input impedance obtained by FEM with and without POD-based MOR.

The accuracy and computational cost of present method are summarized in TABLE I, which contains the count of solutions in the error ranges. We need more than 30 basis vectors for satisfactory results. The computational time for the present method is reduced to 15.9% when *r*=30, about 1% of which is spent for construction of the reduced equation (11).

It is pointed out here that the accuracy depends on the size of ambient region. Hence, we have to carefully determine its size by evaluating the accuracy before the optimization.

2) Optimization at Single Frequency

MLA is optimized at 920MHz by POD-based MOR in which the number of snapshot and basis vectors are set to 30. DoFs of design and ambient region are the same as those mentioned. In the optimization processes, we employ the micro genetic algorithm [11]. The aim of the antenna optimization is realization of MLA whose input impedance is 50Ω and minimization of antenna area *S*. The optimization problem is defined by

$$g_1(\boldsymbol{d}) = \left|Z(\boldsymbol{d}) - 50\right| + 10 \times S(\boldsymbol{d}) \quad \to \min. \tag{16}$$

where $Z(\boldsymbol{d})$ and $\boldsymbol{d}=[d_0, d_1,\ldots, d_5]$ are input impedance of MLA and design parameters.

The optimization results are shown in TABLE II which includes the best and average values for 10 trials with different random seeds. Figure 2 shows antenna shapes obtained by FEM and FEM-MOR. It is found that there are differences in the resultant antenna shapes while their input impedances are nearly 50 ohm. We conclude that the present method can reduce the computational time to about 1/6 without deteriorating the performance of optimization.

B. Spiral Planar Antenna

1) Accuracy and Computational Time

SPA is located in the design region in Fig.1. The shape of SPA is expressed by the design parameter $\boldsymbol{d}=[d_0, d_1,\ldots d_5]^t$ shown in Fig. 3. The domain is again subdivided into design and ambient regions, the former of which includes SPA. The DoFs in the design and ambient regions are 541161 and 1844260, respectively. Our purpose is to have wideband characteristic for SPA. For this reason, we analyze the dependence of SPA on shape and frequencies. In SPA optimization process using present POD-based MOR, we snapshot EM fields changing not only shapes but also frequencies. In this work, we snapshot 30 EM fields each at 3GHz, 3.25GHz and 3.5GHz. In order to validity present POD-based MOR, we analyze SPAs of five different shapes from 3GHz to 3.5GHz at 1GHz interval using FEM and present POD-based MOR. The error is evaluated from eq. (15).

The accuracy and computational cost are summarized in TABLE III. If *r* is set more than 20, all the solutions have numerical errors smaller than 5%. Moreover, the computational cost is less than 17% of the conventional FEM analysis.

2) Optimization of wideband antenna

SPA is optimized to have small return losses in 3.0–3.5GHz. We snapshot the EM fields at 0.25GHz interval, that is, we have snapshots at 3GHz, 3.25GHz and 3.5GHz. Moreover, we snapshot the EM fields for 30 different shapes at these

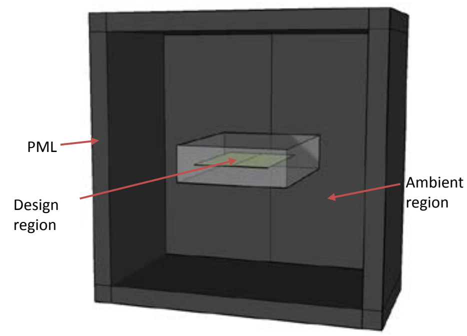

Fig. 1. Numerical model

TABLE I
NUMBER OF SOLUTIONS AND COMPUTATIONAL TIME FOR MLA

Error range	-1.0%	1.0-5.0%	5.0- %	Elapsed time*
r=20	0	0	50	9.3% (60min)
r=30	7	40	2	15.9% (102min)

* Intel(R) Xeon(R) CPU E5-2650(2.6GHz,16cores) is used to compute result in tables I, II and III..

TABLE II
OPTIMIZATION RESULTS OF MLA

	$g_1(\boldsymbol{d})$	$Z(\boldsymbol{d})$ (Ω)	$S(\boldsymbol{d})$ (m^2)	Elapsed time
FEM (best)	0.52	49.6-j0.13	0.022	100% (22620min.)
FEM (average)	3.64	-------	-------	
FEM-MOR (best)	0.90	50.7+j0.11 (*50.9+j0.44)	0.030	17.2% (3891min.)
FEM-MOR(average)	4.62	-------	-------	

* The value is computed by conventional FEM in post processing.

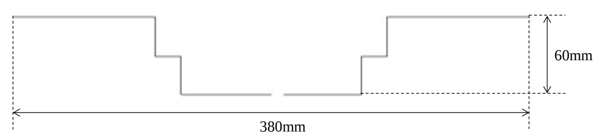

(a) MLA shape obtained by FEM(best).

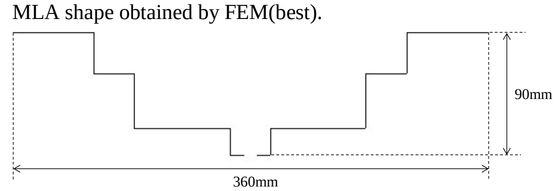

(b) MLA shape obtained by FEM-MOR(best).
Fig. 2 MLA shapes obtained by optimization.

TABLE III
NUMBER OF SOLUTIONS AND COMPUTATIONAL TIME FOR SPA

Error range	-1.0%	1.0-5.0%	5.0- %	Elapsed time
r=5	2	18	10	6.9%(215min.)
r=10	11	14	5	9.7%(302min.)
r=15	19	9	2	12.5%(389min.)
r=20	27	3	0	16.7%(520min.)

frequencies. The aim of the optimization of SPA is minimization of return loss over the frequency range 3.0-3.5GHz. The optimization problem is defined by

$$g_2(\boldsymbol{d}) = \sum_{i=1}^{6} 20\log_{10}\left|\frac{Z_{\text{in}}(\boldsymbol{d}, f_i) - Z_0}{Z_{\text{in}}(\boldsymbol{d}, f_i) + Z_0}\right| \to \min. \tag{17}$$

where Z_0 is 50Ω, $Z_{\text{in}}(\boldsymbol{d}, f)$ is input impedance of SPA and f_1 - f_6 ranges from 3GHz to 3.5Gz at 0.1GHz interval.

In TABLE IV, we summarize the fitness value and design parameter of the optimization results of SPA. There are no significant differences in the resultant fitness values for all values of *r*. Moreover, those fitness values computed by present method are in good agreement with those computed by the conventional FEM in the post processing. Figure 4 shows the manufactured SPA which has the optimized size shown in Table IV. The computed and measured frequency characteristics of the return loss are shown in Fig. 5. It is found that the results obtained by MOR and conventional FEM are in good agreement. There are some discrepancies between the computed and measured results. It is experimentally confirmed, however, that we finally have the desired broadband antenna.

If we perform this optimization using the conventional FEM, we need about 12 hours for one generation in the GA process. On the other hand, we can perform the same computation for 50 minutes using the present MOR when r=5. We conclude that we can perform fast and accurate optimization using the present method.

V. Conclusion

In this paper, the fast optimization method using POD-based MOR which we had proposed has been applied to shape optimization of MLA. We have compared accuracy and computational time between the conventional and present MOR method. It has been shown that the computational time using present method could be reduced to about 17% without deterioration of accuracy. Moreover, we have proposed novel POD-based MOR for optimization of wideband antennas which is applied to optimization of SPA. We also successfully optimize the SPA using the present method and the optimized antenna has been shown to possess the desired wideband property numerically and experimentally.

References

[1] H. Makimura, Y. Watanabe, K. Watanabe, and H. Igarashi, “Evolutional design of small antennas for passive UHF-band RFID,” *IEEE Trans. Magn.*, vol. 47, no. 5, pp. 1510–1513, May 2011.

[2] G. Marrocco, “The Art of UHF RFID Antenna Design : Impedance-Matching and Size-Reduction Techniques,” *IEEE Trans. Antennas Propag.*, vol. 50, no. 1, pp. 66–79, Feb. 2008.

[3] T. Mori, R. Murakami, Y. Sato, F. Campelo and H. Igarashi, “Shape Optimization of Wideband Antennas for Microwave Energy Harvesters Using FDTD,” *Abstract of CEFC2014*, Annecy, France, May, 2014.

[4] S. Burgard, O. Farle and R. D. Edlinger, “A Novel Parametric Model Order Reduction Approach with Applications to Geometrically Parameterized Microwave Devices,” *COMPLE*, vol. 32, no. 5, pp. 1525-1538, 2013.

[5] Y. Sato and H. Igarashi, “Model Reduction Based on the Method of Snapshots for Eddy Current Problems,” *IEEE Trans. Magn*, vol. 49, no. 5, pp. 1697-1700, May, 2013.

[6] T. Henneron and S. Clénet, “Model Order Reduction of Nonlinear Magnetostatic Problems Based on POD and DEI Methods,” *IEEE Trans. Magn*, vol. 50, no. 2, Feb., 2014.

[7] D. Schmidthäusler S. Schöps and M. Clemens, “Linear Subspace Reduction for Quasistatic Field Simulations to Accelerate Repeated Computations,” *IEEE Trans. Magn.*, vol. 50, no. 2, Feb., 2014.

[8] Y. Sato, H. Igarashi, “Model Order Reduction Applied to Optimization of Electromagnetic Devices,” *Proceeding of ISTET2013*, Pilsen, Czech Republic, June, 2013.

[9] J.-P. Berenger, “A perfectly matched layer for the absorption of electromagnetic waves,” *J. Comput. Phys.*, vol. 114, pp. 195–200, 1994

[10] Z. S. Sacks et al., “A perfectly matched anisotropic absorber for use as an absorbing boundary condition,” *IEEE trans. Antennas Propagat.*, vol. 43, pp. 1460-1463, Dec. 1995.

[11] C. A. C. Coello, and G. T. Pulido, “ A micro genetic algorithm for multi objective optimization,” *EMO 2001, LNCS 1993*, pp. 126-140, 2001.

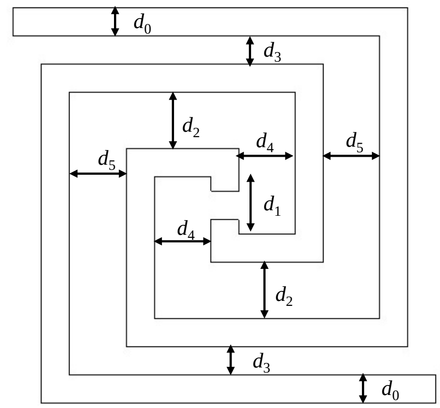

Fig. 3 Spiral antenna characterized by design parameters.

TABLE IV
Optimization results of SPA

	$g_2(\boldsymbol{d})$	Optimized parameters $\boldsymbol{d}$
r=5	-65.3 (-66.4)	$\boldsymbol{d}=[d_0, d_1, d_2, d_3, d_4, d_5]^t$ $=[2,8,13,0,4,6]^t$
r=10	-65.5 (-66.4)	
r=15	-66.8 (-66.4)	
r=20	-66.5 (-66.4)	

* The values in ( ) are computed by conventional FEM in post processing.

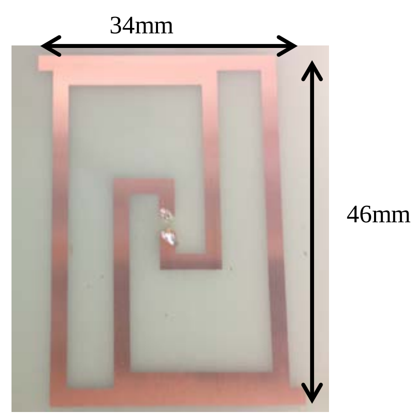

Fig. 4 Manufactured SPA after optimization

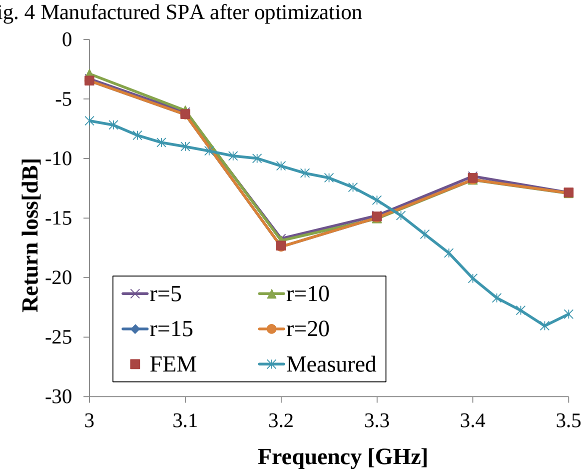

Fig. 5 Return loss of optimized SPA.